Legal Medicine 68 (2024) 102410

Contents lists available at ScienceDirect

Legal Medicine

journal homepage: www.elsevier.com/locate/legalmed

Extracorporeal bullet trajectory determination from scanned phantoms with bullet defects

G.A.J.C. Crombag [a,*], B.J.M. Hofman [b], F. Riva [c,d], P.A.M. Hofman [a], W. Kerkhoff [e]

[a] Department of Radiology & Nuclear Medicine, Maastricht UMC+, Maastricht, the Netherlands
[b] Radboud University, Nijmegen, The Netherlands
[c] Centre universitaire de médicine légale, Université de Lausanne, Switzerland
[d] Ecole des sciences criminelles, Université de Lausanne, Switzerland
[e] Netherlands Forensic Institute, The Hague, the Netherlands

ARTICLE INFO

Keywords:
Shooting incident reconstruction
Bullet trajectory
Computer Tomography
3D trajectory reconstruction
Error estimation

ABSTRACT

Shots with two different calibres (0.32 Auto and 9 mm Luger) were fired through phantoms that simulated human torsos, mounted on undercarriages with witness panels. The perforated phantoms were scanned with computed tomography (Siemens) using 80 kV and 140 kV and a slice thickness of 1 mm. The intracorporeal trajectories in the phantoms were compared to the known extracorporeal trajectories, derived from the perforations in witness panels. The discrepancy between the intracorporeal and extracorporeal trajectories, denoted as the absolute angle, was calculated for the trajectories before (front) and after (rear) the phantoms. Mean absolute angles at the front were lower than at the rear (2.27° vs. 4.54°) and the difference was statistically significant ($p < 0.001$). The results of the study imply that the line between the entrance and the exit wound in a scanned victim can be extended to the extracorporeal bullet trajectory leading towards the entrance wound. The absolute angles presented in this study give an impression of the expected errors with the two calibres. This can be helpful in shooting investigations to assess the position of the shooter from entrance and exit wounds in a scanned victim.

1. Introduction

Previous studies have shown that the use of post-mortem computed tomography (CT) after gunshot incidents results in additional relevant information compared to autopsy [1–3]. A systematic review published in 2019 revealed 59 papers addressing the radiological reconstruction of bullet trajectories within the human body [4]. The included studies show an additional value of post-mortem imaging in case of gunshot injuries to identify bullets, determine caliber and assess trajectories inside bodies. However, more research is necessary to establish the accuracy and precision of the reconstruction of extracorporeal bullet trajectories, extrapolated from wound channels in scanned bodies. The accuracy and precision of methods to determine bullet trajectories from defects in fixed objects is better established. These aspects have been studied with various weapons, impact angles and target materials [5–9]. Studies have also been conducted on bullet deflection through human soft tissue [10–12]. These studies explored the deflection between a bullet's trajectory before and after perforation of phantoms that simulated human soft tissue. This deflection was expressed as the angle between the bullet's original trajectory before impact on the phantom and the trajectory behind the phantom, after perforation. These studies demonstrated that the magnitude of deflection is influenced by bullet type and by the length of the wound channel [10,11]. The influence of impact angle and muzzle-to-target distance were demonstrated to be less important [12]. As explained, these studies explored the relationship between the trajectory of a bullet in air, before and after perforating a phantom. Bullet behavior in these phantoms, or the relationship between the trajectories and the locations of entrance or exit defects in the phantoms was not explored in these studies. Like most studies on bullet behavior in human soft tissue, the phantoms used in these studies were blocks of ballistic gelatine. This material is often used as a simulant for muscle tissue and other subcutaneous soft tissues [13–16]. Aspects like the depth of bullet penetration, the transfer of kinetic energy (roughly equivalent to the bullets potential to cause trauma in tissue) and bullet

* Corresponding author at: Department of Radiology and Nuclear Medicine, Maastricht University Medical Centre, P.O. Box 5800, 6229 HX Maastricht, The Netherlands.
E-mail address: genevieve.crombag@mumc.nl (G.A.J.C. Crombag).

https://doi.org/10.1016/j.legalmed.2024.102410
Received 17 July 2023; Received in revised form 16 December 2023; Accepted 15 January 2024
Available online 17 January 2024

deformation are often studied using this material. Properly prepared ballistic gelatine is homogeneous which makes studies reproducible, allowing results from different studies to be compared [17]. However, the homogeneous nature also makes it less representative of the human body, which consists of multiple tissues with varying densities and mechanical strengths.

The current study was designed to explore the possible discrepancy between the direction of a visualised bullet trajectory in a human body and its extended, extracorporeal, trajectory through air. Knowledge of this possible discrepancy can be used in reconstructing shooting incidents. An extracorporeal bullet trajectory leading from an entrance wound gives information on the direction from which the shot came and thereby on the spatial relationship between the victim and shooter during a shot. An extracorporeal bullet trajectory leading from an exit wound can give information on the body posture and position of a victim on a crime scene, if the respective bullet caused a defect in a fixed object. The current study is conducted by shooting at phantoms mounted on undercarriages with witness panels. The visualised intracorporeal trajectories in the phantoms were compared to the known extracorporeal trajectories, derived from the perforations in witness panels placed before and after the target (phantom). The focus of the study is put on the magnitude of the discrepancy between the trajectories derived from the intracorporeal trajectories on the one hand and the known trajectories on the other. This magnitude can be used to estimate the uncertainty around extracorporeal trajectories in forensic casework, derived from scanned bullet wounds in soft tissue. Because of the limited amount of data, the direction of the discrepancy (any tendency to deflect in a certain direction) was not analysed in detail.

2. Materials and methods

2.1. Weapons and ammunition

The number of weapon/ammunition combinations that can be encountered in forensic casework, in terms of different firearm models and ammunition brands, is huge. However, some classes of weapon/ammunition combinations have a similar ballistic performance in terms of wounding effect. For the current study, two classes were chosen that are commonly encountered in forensic casework in Switzerland and The Netherlands. The first is a combination of 0.32 Auto calibre firearms, firing 4.7 g full metal jacket round nose (FMJ-RN) bullets. The second is a combination of 9 mm Luger calibre firearms, firing 7.5 g full metal jacket round nose (FMJ-RN) bullets. As a representative of the first combination, 0.32 Auto bullets (4.75 g FMJ-RN) were fired with a mean velocity of 308 m/s from a Skorpion Vz61 sub-machinegun, generating a mean kinetic energy of 225 J. As a representative of the second combination, 9 mm Luger bullets (7.5 g FMJ-RN) were fired with a mean velocity of 363 m/s from a Glock Gen 5 model 17 pistol, generating a mean kinetic energy of 494 J. The combinations will simply be designated with their respective calibres 0.32 Auto and 9 mm Luger in the paper.

2.2. Phantoms

The phantoms were designed to:

- allow full bullet perforation of the selected bullets, causing both an entrance and an exit defect;
- fit through the 78 cm diameter of the used CT scanner when mounted on an undercarriage with witness panels.
- be free of metal, to avoid a beaming effect in the scans;
- have a ballistic resistance close to human soft tissue and have a non-homogenous nature, causing realistic intracorporeal bullet behaviour;
- keep their original shape and position when shot, with the noted exception of receiving a bullet channel that could be visualised on a CT-scan.

The phantoms were constructed from leather, ballistic gelatine and porcine liver. The leather served as a skin simulant and consisted of 1 mm thick chrome tanned cowhide with a synthetic finish. The use of tanned cowhide as a proxy for human skin in ballistic research was first described by Jussila et. al [14]. The phantom was filled with gelatine and porcine liver. The gelatine was prepared according to Jussila [13]. The porcine liver was added to the molten gelatine to decrease the overall homogeneous nature of the phantom's interior. Imbedding tissue in gelatine for the purpose of ballistic research was first described by Lewis et. al [18].

The leather was used to construct the side walls of elliptical cylinders. The bottom of the cylinders consisted of a 0.5 cm thick elliptical PVC plate, measuring 35x25 cm, that was attached to the leather side walls. The height of the leather cylinders was 25 cm. The cylinders were held upright, with their finished sides outward, by a PVC structure that was open at the top. A quantity of 15 kg of molten, 10 % ballistic gelatine with a temperature between 45 and 40 °C was poured in each cylinder. A mass of approximately 8 to 10 kg of porcine liver per phantom was immersed in the gelatine. The liquid gelatine was partially absorbed by the rough inner side of the leather and adhered to the gelatine as it cooled down and solidified. Combined, the leather, liver and solidified gelatine formed elliptical/cylindrical phantoms measuring roughly 35 × 25 × 25 cm in size and weighing between 23 and 25 kg. The mass of gelatine and liver caused the leather to bulge a little beyond the original 25 × 35cm dimensions, especially at the bottom. Both the elliptical PVC bottom plates of the phantoms and the PVC structures that held the phantoms upright were attached to 100 × 42 × 6 cm PVC undercarriages. Each undercarriage was provided with two 32x39cm frames attached at the far ends, that allowed attachment of paper witness panels. Because of the rigid, boxlike nature of the undercarriages and the elastic nature of PVC and gelatine, the phantoms could absorb kinetic energy, while retaining their original positions relative to the frames and witness panels. Three phantoms each were prepared per weapon/ammunition combination. The phantoms were stored in a cooled storage room, set at 4 °C for 24 h prior to shooting.

2.3. Shooting protocol

A paper witness panel was attached to the front and back frame. Four bullets were fired through each phantom. Seen from the shooter, the first shot was fired through the top left side of the front witness panel and subsequently through the top left side of the phantom. The bullet exited the phantom and caused a defect in the back witness panel. The bullet defects in the front witness panel and in the front of the phantom (entrance side) were both marked 'A'. The bullet defects in the back of the phantom (exit) and in the back witness panel were both marked 'B'. Together, this shot will be referred to as shot A-B, see Fig. 1.

Shot C-D was fired through the bottom left but more to the centre of both the front witness panel and phantom. Shot E-F was fired to the right of the phantoms centre, next to and approximately at the same height as shot C-D. Shot G-H was fired through the top right side of the front witness panel and through the top right side of the phantom, at approximately the same height as shot A-B. The defects were marked after each shot to avoid mix-ups. Because the shots A-B and G-H were fired through the sides of the elliptical phantoms and the shots C-D and E-F were fired more through the centres, trajectories A-B and G-H are shorter than trajectories C-D and E-F in all phantoms. Another difference between trajectories is that the bullets from trajectories A-B and G-H entered and exited the phantom at an angle. The bullets from trajectories C-D and E-F entered and exited more or less orthogonal.

After completing the four-shot sequence on each phantom, the distance from the defects in the witness panels to the sides of the PVC

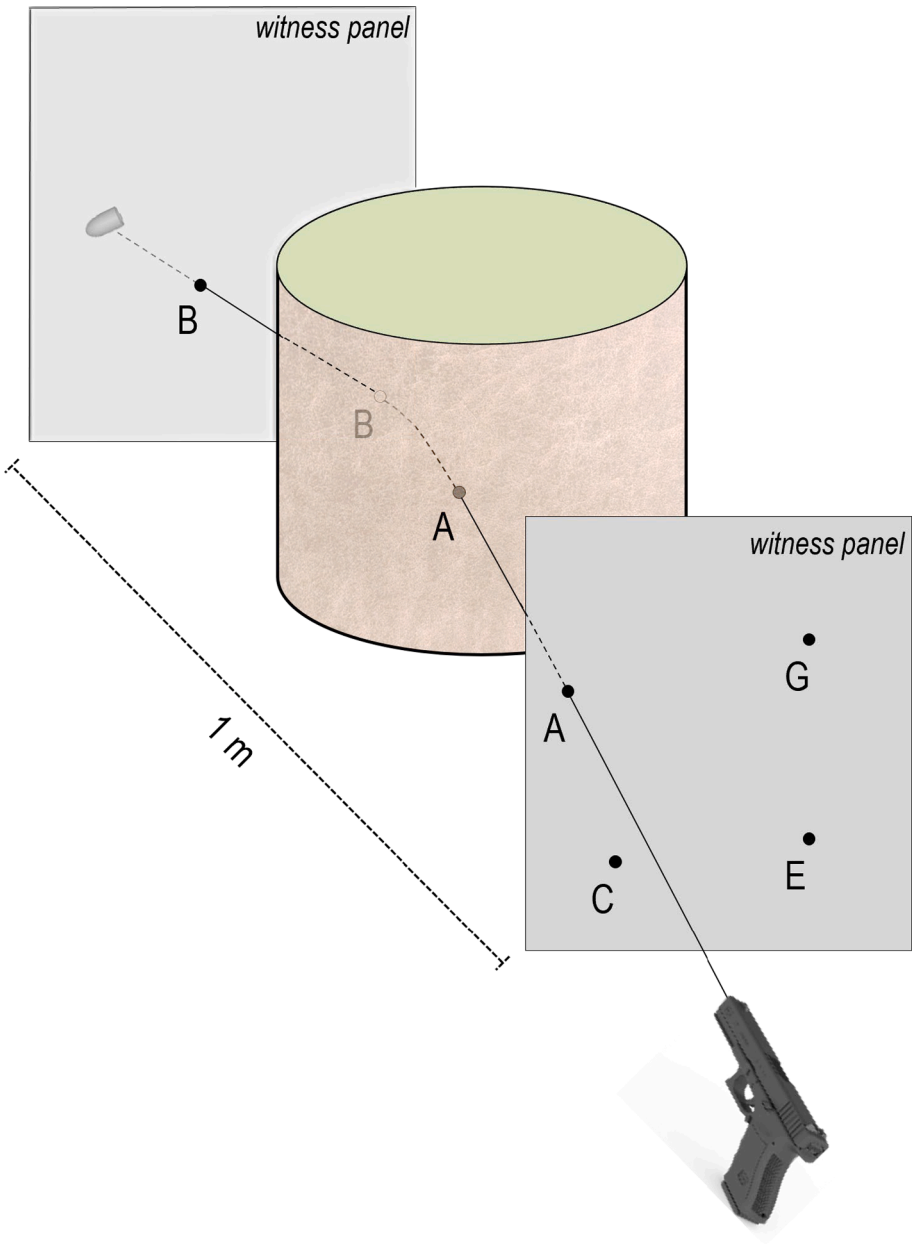

Fig. 1. Visualisation of the set-up of the experiment. Sketch of a phantom, on its undercarriage with witness panels, when shot. For clarity, details like the PVC struts and side-mounts that supported the phantom and witness panels are not included. This figure visualizes how the defects caused by shot A-B in the witness panels and phantom were marked. The figure also visualizes the markings C, E and G on the front witness panel to illustrate shot placement. To avoid complicating the figure, the markings D, F and H on the exit side of the phantom and on the rear witness panel were not visualised.

frames were measured. The defects in the papers consisted of star-shaped ruptures. The centre of each defect could be reconstructed by folding the paper back in its original position. The bottom parts of the frames were used as the x-axes. The left vertical sides (seen from the shooter) of both frames were used as the y-axes. Because the paper on the front frame extended beyond the frame and the first (top left) shot was fired left of the frame, the y-values on the front witness panel for all A-B shots are negative. All other x- and y-values are positive. After shooting and measuring the x- and y-values, the witness panels were removed and the phantoms, mounted on the undercarriages with the PVC frames that had held the witness panels in place, were transported in cooled condition and scanned. Time between shooting and scanning was approximately 3–5 h.

2.4. Scanning protocol

All phantoms were scanned using computed tomography (Somatom Force; Siemens Healthineers, Forchheim, Germany). Scans were performed at 140 kV using a tube current of 203 mAs and a slice thickness of 1 mm. Image data sets were reconstructed using a bone and soft tissue reconstruction kernel. The generated imaging data sets were analysed using a dicom viewer software (Horos, Horosproject.org). Assessment was performed using multi-planar reconstruction (MPR) and volume rendering techniques. Every entrance and exit defect in the phantom was identified and compared to the marked four-shot sequence, which allowed visualization of the short trajectories (A-B and G-H, Fig. 2A) and long trajectories (C-D and E-F, Fig. 2B) through the phantom. The software allowed identification of every entrance and exit wound by means of a coordinate (x, y, z). Also the coordinates of the corners of bottom

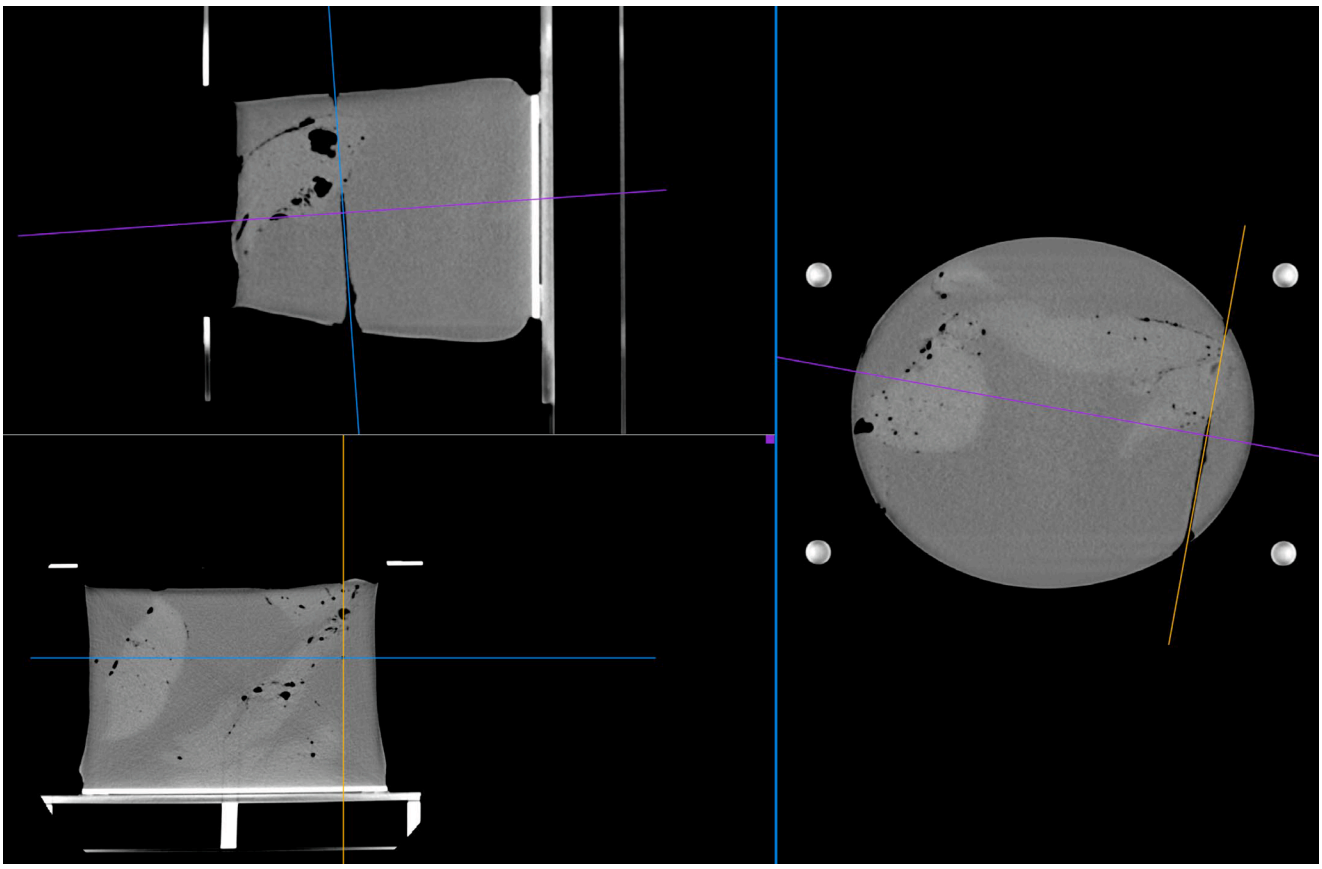

Fig. 2A. Example of CT data using MPR *Example of analysing CT data using multi-planar reconstruction (MPR) in Horos. The top left part of the figure depicts a side view of a phantom (tilted sideways). The axis lines indicate bullet path G-H through the phantom, seen from different sides. The bottom left part and the right part of the figure depict the front and top view respectively of the same phantom and bullet path. From a visual assessment, the bullet's path through the gelatine and imbedded liver has been a straight line.*

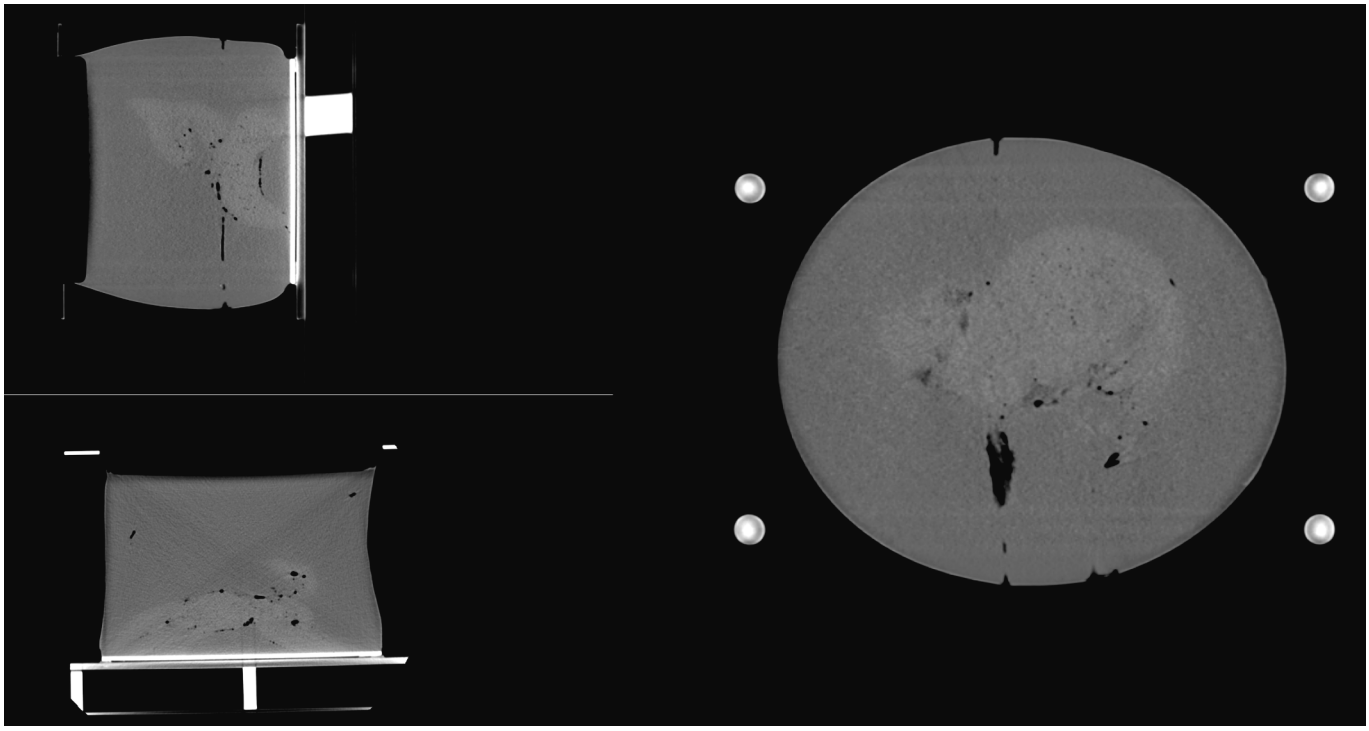

Fig. 2B. Again a side (top left), front (bottom left) and top (right) view of a phantom, with bullet path C-D. The axis lines have been omitted to better visualise the path. The visual assessment (most notably with the side view) indicates that the bullet followed a straight line through the gelatine and liver.

horizontal and left vertical side (seen from the shooter) of both witness frames were determined.

2.5. Angle measurement

Using the obtained coordinates, the absolute angles were calculated for each trajectory. The absolute angle is the measure of the bullet's deflection, and describes the angle between two lines: the true trajectory, being the line between the defect in the phantom and the associated defect in the witness panel, and the line extended between the entrance and exit defect in the phantom. See Fig. 3 for a schematic overview of these angles. For each trajectory, two absolute angles were calculated, on the front and on the back of the phantom (entry angle and exit angle).

The coordinates of the defect in the front and rear witness panel were expressed as coordinates in the CT-scan space. All coordinates were collected in a data sheet consisting of 24 samples each containing 4 sets of coordinates for each trajectory (physical front witness panel defect, phantom entrance defect, phantom exit defect, rear witness panel defect). These coordinates represent the bullet trajectories. Using the python library SymPy (docs.sympy.org/latest/index.html), a robust mathematics library, the 4 coordinates of each trajectory were loaded into a simulated 3D space. In this space coordinates of the of the intersection of the extended trajectory through the phantom and the front and rear witness panel were calculated. The absolute angle was calculated by rebasing both the projected and the actual vector on the phantom entry point first, and then taking their dot product. This angle was verified using the remaining two angles of the vector triangle formed by the phantom entrance defect, the physical witness panel defect and the projected witness panel defect.

2.6. Statistics

Significant differences in absolute angle between the two calibres and between the short and long trajectories were tested using an independent samples T-test. P-values < 0.05 were considered to indicate statistical significance. SPSS (version 25, International Business Machines, Armonk, New York, USA) was used for the statistical analyses.

3. Results

For every phantom the intracorporeal trajectory for the four fired shots could be identified, which resulted in a total of 24 trajectories. A visual assessment of the trajectories in the phantoms did not support the prior assumption that the inhomogeneous content of the phantoms would cause bullet deflection. All trajectories appeared as straight lines, independent of their lengths and independent of whether or not a pork liver was perforated (see Fig. 2A/2B).

The calculated absolute angles demonstrate lower values in the front of the phantom (front witness panel to entrance defect, mean 2.27°) compared to the back of the phantom (exit defect to rear witness panel, mean 4.54°) ($p < 0.001$) (tables 1 and 2).

There was no significant difference in absolute angle between the used calibre or between the short and long trajectories at the front of the witness panel (respectively $p = 0.60$ and $p = 0.995$). At the rear witness panel there was also no significant differences in absolute angle between the used calibre ($p = 0.57$). A distribution of the absolute angles (and projection angles) in a polar plot is shown in Figs. 4 and 5 for the front and rear witness panel respectively. However, there was a significant difference in absolute angle at the rear witness panel between the short and long trajectories ($p < 0{,}001$), where the shorter and angled trajectories showed a greater absolute angle (mean 5.7°) compared to the longer and orthogonal trajectories (mean 3.3°) (tables 1 and 2).

Table 1
Front and rear absolute angles for the 0.32 auto calibre.

Trajectory	Trajectory length	Length channel inside phantom (cm)	Front absolute angle	Rear absolute angle
1	Short	13.91	1.46	5.83
2	Long	27.98	2.11	3.70
3	Long	28.88	2.33	3.45
4	Short	18.05	1.20	5.92
5	Short	17.87	2.04	5.90
6	Long	26.32	2.03	3.81
7	Long	28.82	1.26	4.15
8	Short	13.03	1.39	5.60
9	Short	18.33	0.69	7.29
10	Long	27.59	1.80	3.92
11	Long	29.53	2.92	2.63
12	Short	14.76	0.73	4.44
Mean			1.66	4.72
STDEV			0.66	1.36

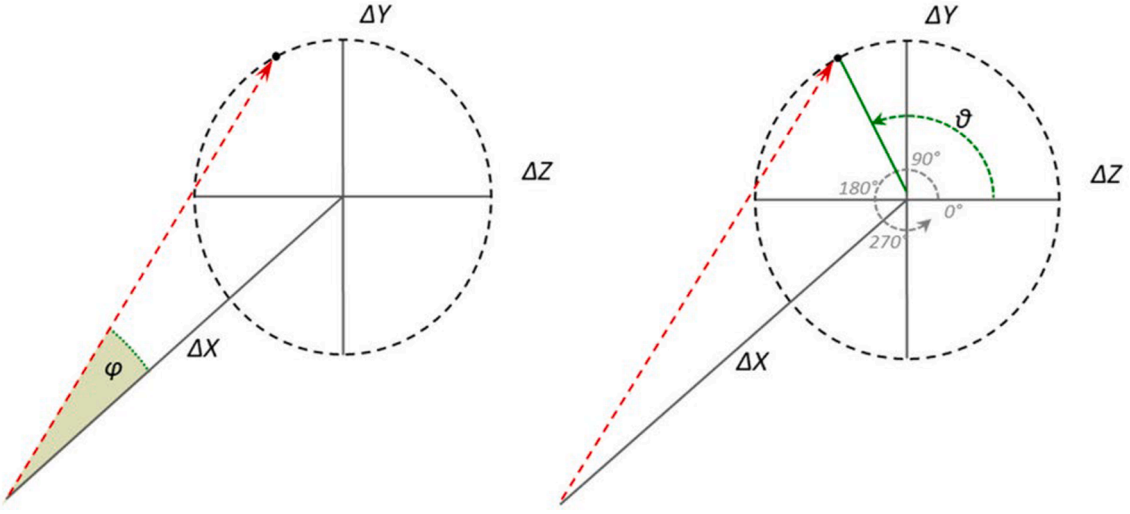

Fig. 3. Schematic overview angles [10] Difference between the absolute angle on the left and the projection angle on the right. The absolute angle is a measure for the magnitude of deflection while the projection angle is a measure for the direction of deflection. The absolute angle (magnitude) is the focal point of the study and is analysed in detail. An impression of the projection angle (direction) of the deflection is given in Figs. 4 and 5.

Table 2
Front and rear absolute angles for 9 mm calibre.

Trajectory	Trajectory	Trajectory length (cm)	Front absolute angle	Rear absolute angle
1	Short	14.95	1.55	5.44
2	Long	26.46	1.60	4.95
3	Long	28.99	4.54	1.18
4	Short	15.65	7.05	6.21
5	Short	13.04	6.06	6.66
6	Long	26.95	0.42	1.53
7	Long	29.43	2.30	4.25
8	Short	15.68	1.28	6.04
9	Short	20.30	2.47	4.34
10	Long	25.84	3.14	3.09
11	Long	29.32	2.81	3.44
12	Short	15.46	1.39	5.11
Mean			2.88	4.35
STDEV			2.02	1.76

4. Discussion

The ultimate aim of this study was to provide data for the reconstruction of shooting incidents. The front absolute angle provides information on the spatial position of the shooter in relation to the victim and the rear absolute angle provides information on the spatial position of the victim in relation to possible defects in fixed objects in a crime scene. The present study demonstrates significant smaller absolute angles at the front witness panel compared to the rear witness panel and revealed a significant difference in absolute angles between shots fired at an angle at the phantom and with a short trajectory inside the phantom compared to shots fired near-orthogonal and with a long trajectory inside the phantom at the rear witness panel. The result that the mean absolute angle at the rear was significantly higher for the short, angled trajectories than for the long, near-orthogonal trajectories is in apparent contrast to results found in a study by Kerkhoff et al. in 2018 [7]. In that study, the length of the channels appeared to be of more influence on bullet deflection, with both 0.32 Auto and 9 mm Luger bullets, than the impact angle. It must be noted that the impact angle was kept at a constant 45° in study, while the impact angles varied in the current study [7].

The discrepancy between the extracorporeal trajectories derived from the intracorporeal trajectories on the one hand and the known trajectories on the other are indicative of some deflection from the bullet's original trajectory. If the bullets had followed a perfectly straight line, no discrepancy was to be expected, resulting in absolute angles close to 0. In Kerkhoff et al. in 2023 measured deflection angles between 5.7° and 7.4°, for 9 mm Luger bullets going through 23 to 24 cm of gelatine [19]. A visual assessment of high-speed footage lead the authors of that study to remark that: "*Subjectively, deflection starts just before or around the first energy transfer peak, when the bullet's path seems to receive a nick*". This first energy transfer peak occurred at a depth of 16 to 18 cm. This is shorter than most trajectory lengths in the current study. However, the visual assessment of the CT-data indicated that the bullets followed a straight line through the gelatine and liver (see Figs. 2A and 2B). It is therefore not clear where or how the discrepancy between the extracorporeal trajectories and the intracorporeal trajectories is caused. One explanation might be the skin simulant. The leather that was used has a higher mechanical strength than the gelatine and liver. Therefore, deflection might be caused when entering or exiting the phantoms. Another possibility is that a small deflection in the phantoms does occur but is overlooked. The mean discrepancy between the

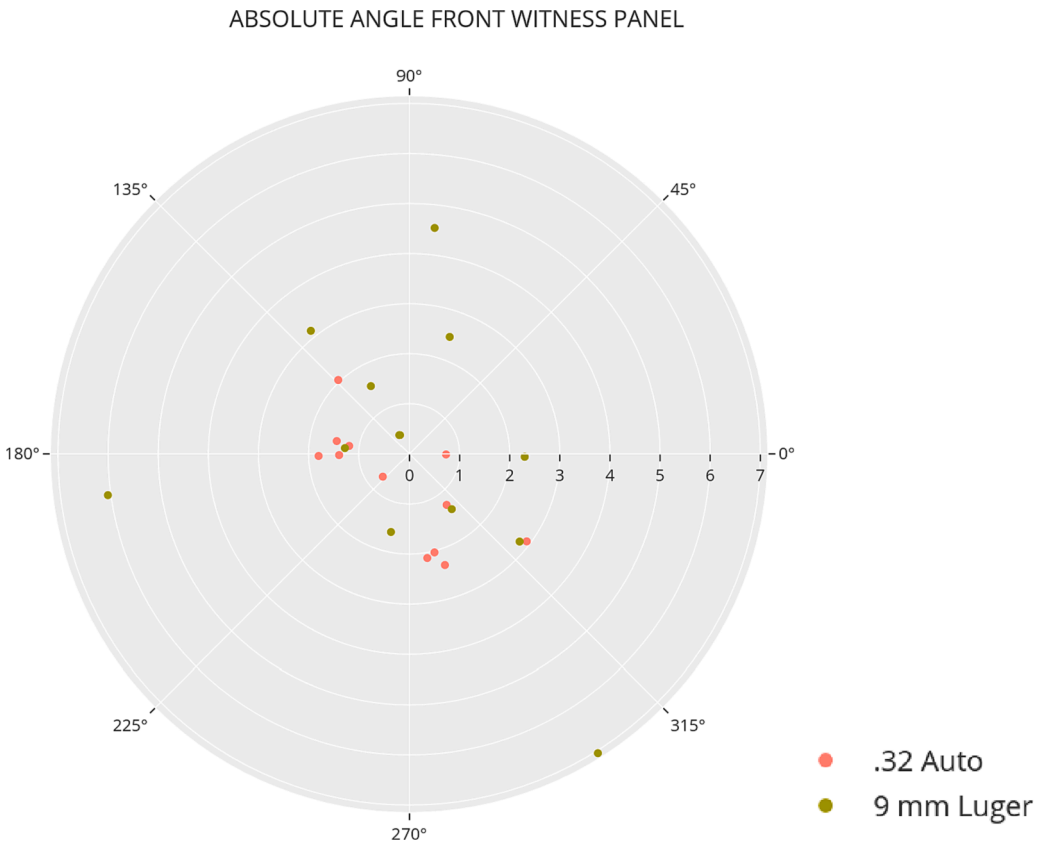

Fig. 4. Polar plot demonstrating the distribution of the absolute and projection angles for each calibre (0.32 Auto in orange, 9 mm Luger in green) for the front witness panel. For clarity of the figure, no distinction is made between the short, angled trajectories and the long, near-orthogonal trajectories. Angles at the front were not significantly different for the short, angled trajectories and for the long, near-orthogonal trajectories. (For interpretation of the references to colour in this figure legend, the reader is referred to the web version of this article.)

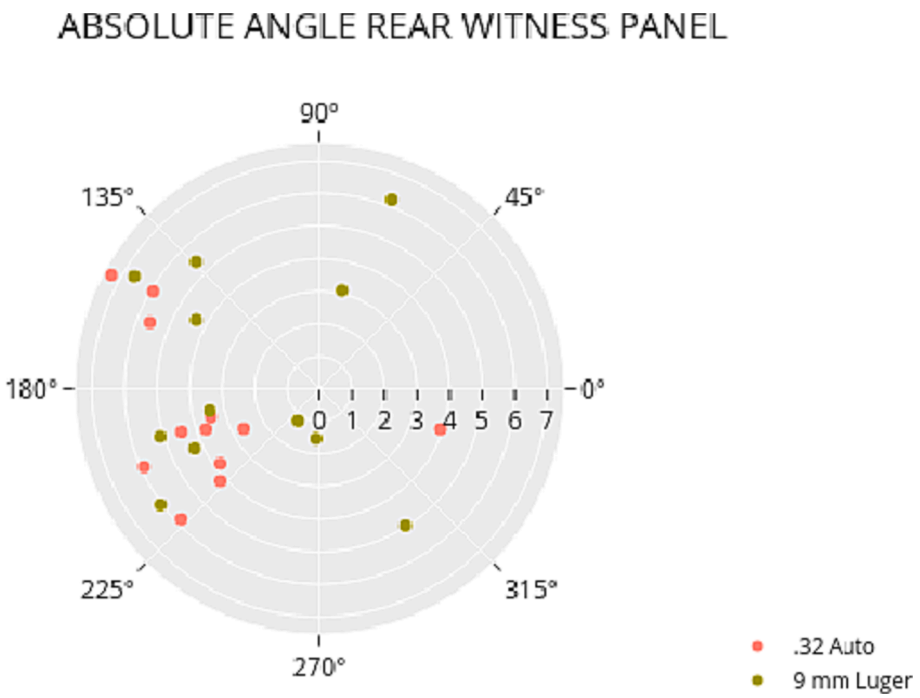

Fig. 5. Polar plot demonstrating the distribution of the absolute and projection angles for each calibre (0.32 Auto in orange, 9 mm Luger in green) for the rear witness panel. For clarity of the figure, no distinction is made between the short, angled trajectories and the long, near-orthogonal trajectories. Angles at the rear were (significantly) higher for the short, angled trajectories than for the long, near-orthogonal trajectories.

extracorporeal trajectories and the intracorporeal trajectories at the front of the phantoms was 1.66 and 2.88 for the two calibers respectively. Whether such a small deviation is discernible when visually assessing CT-data, is not known. A combination of causes is also possible.

The interpretation of these results describing small absolute angles at the front witness panel, imply that the trajectory from inside the phantom, can be extended to the extracorporeal trajectory with a limited range of uncertainty. This can be helpful in shooting investigations to assess the position of the shooter more accurately. Taking the maximum front absolute angle for a 9 mm Luger calibre bullet from table 2 as an example, the 7.05° would result in an approximately 1.24 m error on the estimated shooter position at a distance of 10 m. In the same way these results can be used to assess the position of a victim in a crime scene. The values in tables 1 and 2 can be used as a measure for the expected error on an extended trajectory, with the respective calibres and bullet types.

The phantoms and undercarriages were designed to keep their original form and were scanned in the same position as when shot. Therefore, errors caused by a change of shape of the phantoms, between the moment of bullet passage and the moment of scanning were minimized. This source of error cannot be ignored when assessing bullet trajectories in human bodies in forensic casework. As a rule, a deceased victim of a shooting incident is scanned in a different position than it had when shot. When a person was e.g. shot while standing upright and scanned in supine position, the altered direction of gravitational pull might cause a shift of soft tissues. The magnitude of the shift might be dependent on Body Mass Index [20]. This aspect is left out of scope in the current study, but should be taken into account when reconstructing a shooting incident.

5. Conclusion

The results of this study imply that the line between the entrance and the exit wound in a scanned victim can be extended to the extracorporeal bullet trajectory leading towards the entrance wound with a relatively low amount of uncertainty. The absolute angles presented in this study give an impression of the expected errors on an extended trajectory with the two used calibres. This can be helpful in shooting investigations to assess the position of the shooter from entrance and exit wounds in a scanned victim.

6. Compliance with ethical standards

Funding: This research did not receive any specific grant from funding agencies in the public, commercial, or not-for-profit sectors.

Ethical approval: The used porcine livers were food-grade and stemmed from pigs, slaughtered in accordance with Dutch legislation

Informed consent: Not applicable.

Declaration of competing interest

The authors declare that they have no known competing financial interests or personal relationships that could have appeared to influence the work reported in this paper.

References

[1] R.A.T. van Kan, et al., Post-mortem computed tomography in forensic investigations of lethal gunshot incidents: is there an added value? Int. J. Leg. Med. 133 (6) (2019) 1889–1894.
[2] M.A. Andenmatten, M.J. Thali, B.P. Kneubuehl, L. Oesterhelweg, S. Ross, D. Spendlove, S.A. Bolliger, Gunshot injuries detected by post-mortem multislice computed tomography (MSCT): a feasibility study, Leg. Med. (Tokyo) 10 (6) (2008) 287–292.
[3] F. Makhlouf, V. Scolan, G. Ferretti, C. Stahl, F. Paysant, Gunshot fatalities: correlation between post-mortem multi-slice computed tomography and autopsy findings: a 30-months retrospective study, Leg. Med. (Tokyo) 15 (3) (2013) 145–148.
[4] A. Giorgetti, C. Giraudo, A. Viero, M. Bisceglia, A. Lupi, P. Fais, E. Quaia, M. Montisci, G. Cecchetto, G. Viel, Radiological investigation of gunshot wounds: a systematic review of published evidence, Int. J. Leg. Med. 133 (4) (2019) 1149–1158.
[5] E.J. Mattijssen, W. Kerkhoff, Bullet trajectory reconstruction - Methods, accuracy and precision, Forensic Sci. Int. 262 (2016) 204–211.
[6] M. Walters, E. Liscio, The Accuracy and Repeatability of Reconstructing Single Bullet Impacts Using the 2D Ellipse Method, J. Forensic Sci. 65 (4) (2020) 1120–1127.

[7] W. Kerkhoff, A. Bolck, I. Alberink, E.J.A.T. Mattijssen, R. Hermsen, F. Riva, Pistol bullet deflection through soft tissue simulants, Forensic Sci. Int. 289 (2018) 270–276.
[8] G. Haag, The accuracy and precission of trajectory measurements, AFTE Journal 40 (2008) 145–182.
[9] M. G. Haag, L.C.H., *Shooting incidents reconstruction.* Academic Press San Diego, 2011.
[10] F. Riva, W. Kerkhoff, A. Bolck, E.J.A.T. Mattijssen, Possible influences on bullet trajectory deflection in ballistic gelatine, Forensic Sci. Int. 271 (2017) 107–112.
[11] F. Riva, E. Mattijssen, W. Kerkhoff, Rifle bullet deflection through a soft tissue simulant, Forensic Sci. Int. 291 (2018) 199–206.
[12] W. Kerkhoff, E. Mattijssen, F. Riva, Influence of bullet type and muzzle-to-target distance on trajectory deflection through a soft tissue simulant, Forensic Sci. Int. 311 (2020) 110289.
[13] J. Jussila, Preparing ballistic gelatine–review and proposal for a standard method, Forensic Sci. Int. 141 (2–3) (2004) 91–98.
[14] J. Jussila, A. Leppäniemi, M. Paronen, E. Kulomäki, Ballistic skin simulant, Forensic Sci. Int. 150 (1) (2005) 63–71.
[15] E.J.A.T. Mattijssen, I. Alberink, B. Jacobs, Y. van den Boogaard, Preservation and storage of prepared ballistic gelatine, Forensic Sci. Int. 259 (2016) 221–223.
[16] B. P. Kneubuehl. R. M. Coupland, M.A.R., M. J. Thali, *Wound ballistics - Basics and applications.* Translation of the revised third german edition 2011.
[17] D.J. Carr, T. Stevenson, P.F. Mahoney, The use of gelatine in wound ballistics research, Int. J. Leg. Med. 132 (6) (2018) 1659–1664.
[18] R.H. Lewis, M.A. Clark, K.J. O'Connell, Preparation of gelatin blocks containing tissue samples for use in ballistics research, Am. J. Forensic Med. Pathol. 3 (2) (1982) 181–184.
[19] W. Kerkhoff, et al., The influence of impact velocity on bullet trajectory deflection through ballistic gelatine, Forensic Sci. Int. 346 (2023) 111675.
[20] F. Riva, U. Buck, K. Bußе, R. Hermsen, E.J.A.T. Mattijssen, W. Kerkhoff, Error estimation on extracorporeal trajectory determination from body scans, Int. J. Leg. Med. 136 (3) (2022) 729–737.